# Supporting Information

## Inter-Overlapped $MoS_2$/C composites with Large-Interlayer-Spacing for High-Performance Sodium-Ion Batteries

Yinghui Wang,[a] Ya Yang,[a] Deyang Zhang,[a*] Yangbo Wang,[a] Xiaoke Luo,[c] Xianming Liu,[d] Jang-Kyo Kim[e] and Yongsong Luo[a,b*]

[a] *Key Laboratory of Microelectronics and Energy of Henan Province, Henan Joint International Research Laboratory of New Energy Storage Technology, School of Physics and Electronic Engineering, Xinyang Normal University, Xinyang 464000, P. R. China.*

[b] *College of Physics and Electronic Engineering, Nanyang Normal University, Nanyang 473061, China.*

[c] *School of Information Engineering, Zhengzhou University, Zhengzhou 450001, P. R. China.*

[d] *College of Chemistry and Chemical Engineering, Luoyang Normal University, Luoyang 471934, P. R. China.*

[e] *Department of Mechanical and Aerospace Engineering, Hong Kong University of Science and Technology, Clear Water Bay, Kowloon, Hong Kong, P. R. China.*

[*] Corresponding author. Tel./fax: +86 376 6390801, E-mail: ysluo@xynu.edu.cn (Y. S. Luo), zdy@xynu.edu.cn.

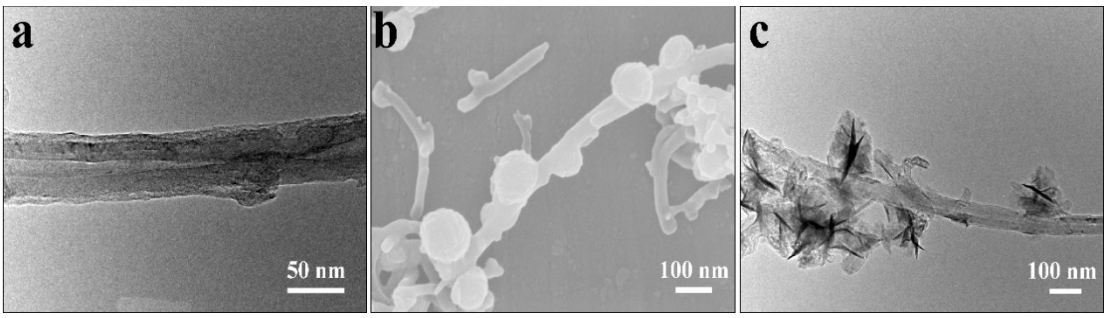


**Fig. S1** (a) TEM image of the CNT@NCT. (b, c) SEM and TEM image of the CNT@NCT@$MoS_2$**.**

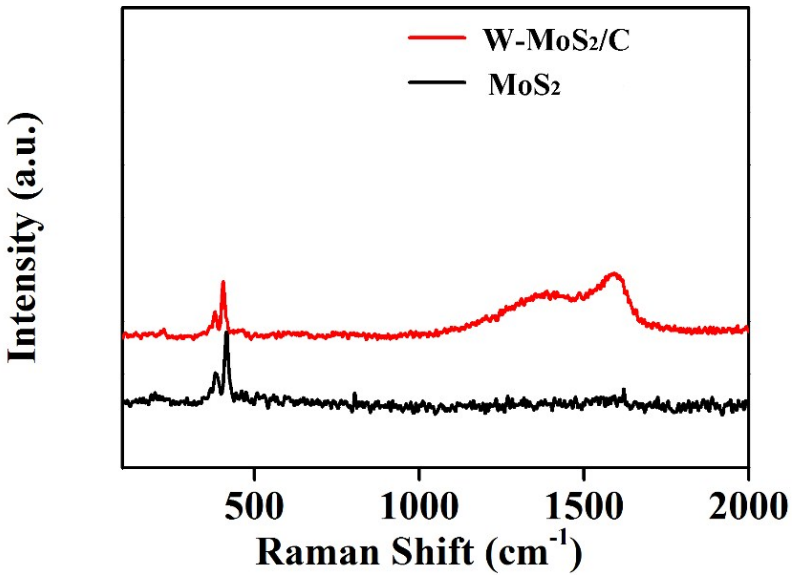


**Fig. S2** Raman spectra of the $MoS_2$ and W-$MoS_2$/C.

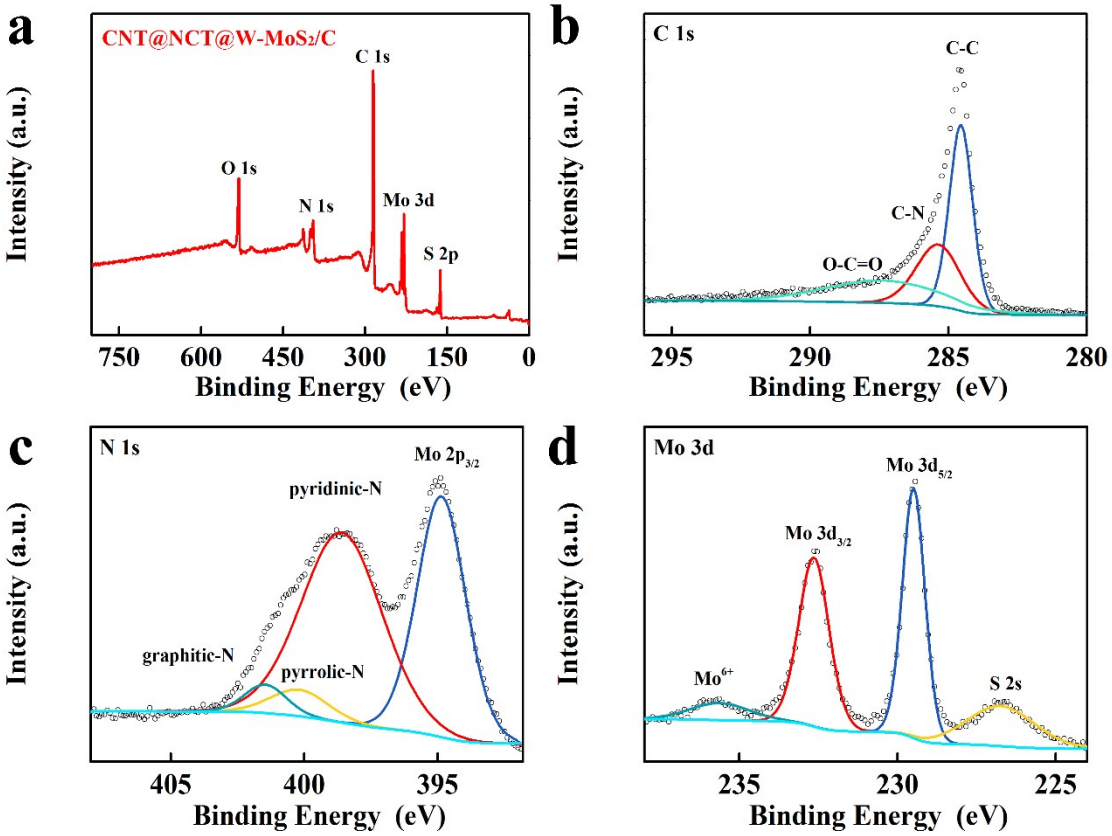


**Fig. S3** (a) XPS survey spectrum of the CNT@NCT@W-$MoS_2$/C. (b-d) High-resolution XPS spectra of the C 1s peak, N 1s peak, and Mo 3d peak in the CNT@NCT@W-$MoS_2$/C.

**Table. S1** Elemental compositions of CNT@NCT@W-$MoS_2$/C composites.

| Element | C | N | S | Mo |
|---|---|---|---|---|
| CNT@NCT@W-$MoS_2$/C | 79% | 3.3% | 11.6% | 6.1% |

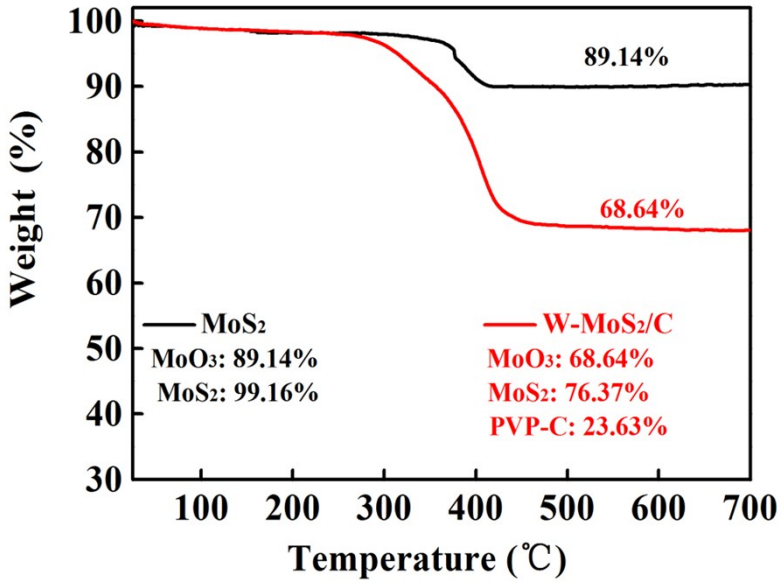


**Fig. S4** TG curves of the $MoS_2$ and W-$MoS_2$/C.

The $MoS_2$ content in the CNT@NCT@W-$MoS_2$/C, W-$MoS_2$/C and pure $MoS_2$ was obtained by heating in oxygen atmosphere from room temperature to 700 °C. First, according to Fig. S4, it can be seen that $MoS_2$ starts to change to $MoO_3$ at around 370 °C, the mass ratio of $MoS_2$ in W-$MoS_2$/C can be calculated using Equation (1). And the ratio of PVP-C to $MoS_2$ in W-$MoS_2$/C is 1:3.2.

$$MoS_2\,(wt\,\%) = \frac{Molecular\ mass\ of\ MoS_2}{Molecular\ mass\ of\ MoO_3} \times\ total\ residual\ weights \times 100\,\% \qquad (1)$$

According to the TG curve of the CNT@NCT@W-$MoS_2$/C (Fig. 3d), it showed a major weight loss at between 270 °C and 600 °C, during which, the carbon component was completely removed by $O_2$ oxidation and $MoS_2$ was oxidized completely to $MoO_3$. Known by Equation (1), the $MoS_2$, PVP-C and CNT@NCT content is 42.89 %, 13.27 %, and 43.84 %, respectively.

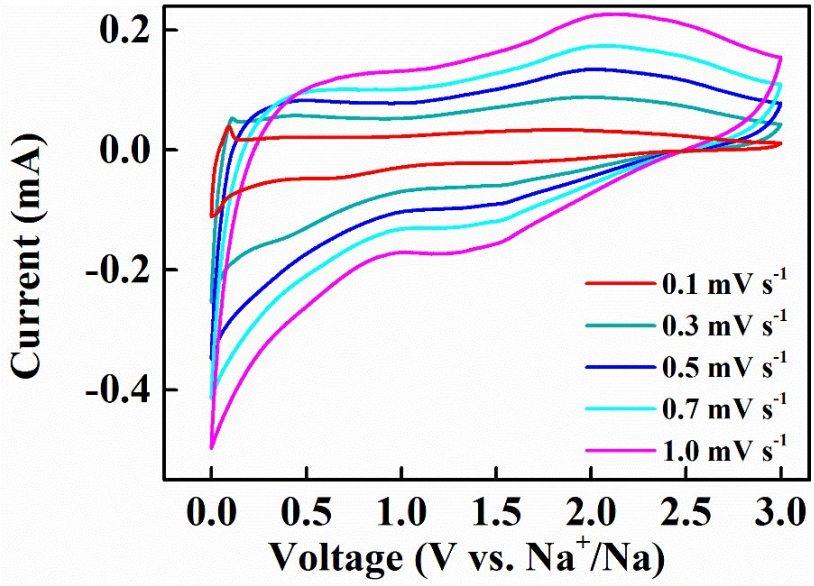


**Fig. S5** Typical CV curves of the CNT@NCT@W-$MoS_2$/C cathode.

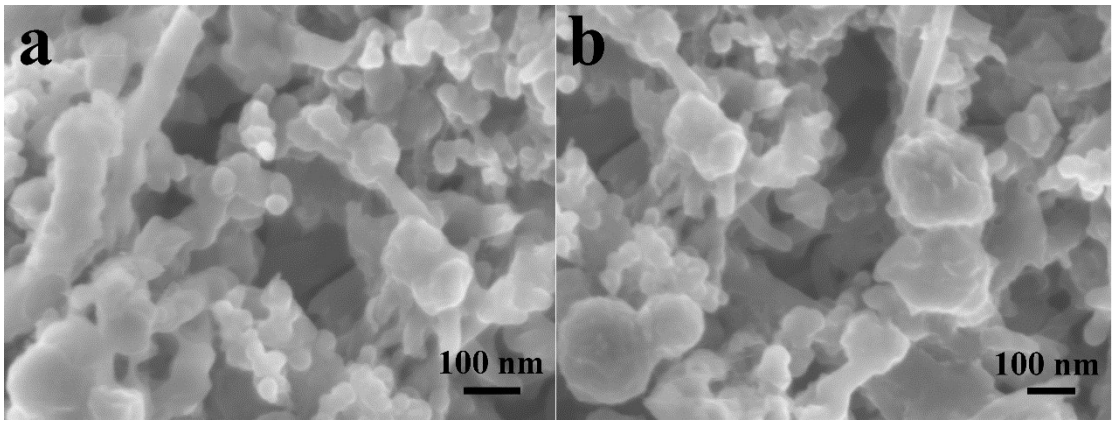


**Fig. S6** (a, b) SEM images of CNT@NCT@W-$MoS_2$/C electrode after 200 cycles at 1 A $g^{-1}$.

**Table S2.** A comparison of the rate capability between this work and the work previously reported in literature.

| Samples | Current density /mA $g^{-1}$ | Cycle number /n | Maintained capacity /mA h $g^{-1}$ | Reference |
|---|---|---|---|---|
| $MoS_2$-$Li_4Ti_5O_{12}$ | 1200 | 200 | 101 | 1 |
| $MoS_2$ nanosheets | 320 | 100 | 251 | 2 |
| $MoS_2$/carbon fibers | 1000 | 100 | 181 | 3 |
| PEO-$MoS_2$ composites | 670 | 70 | 150 | 4 |
| $MoS_2$/rGO composites | 50 | 100 | 203 | 5 |
| 60$MoS_2$ | 25 | 20 | 218 | 6 |
| $MoS_2$/Graphene composites | 320 | 300 | 227 | 7 |
| $MoS_2$ nanowires | 100 | 200 | 200 | 8 |
| $Mo(Se_{0.85}S_{0.15})_2$:CNT | 2000 | 100 | 40 | 9 |
| G-C@$MoS_2$ | 100 | 100 | 155 | 10 |
| CNT@NCT@$MoS_2$/C | 1000 | 136 | 90 | Control sample |
| CNT@NCT@W-$MoS_2$/C | 1000 | 200 | 256 | This work |

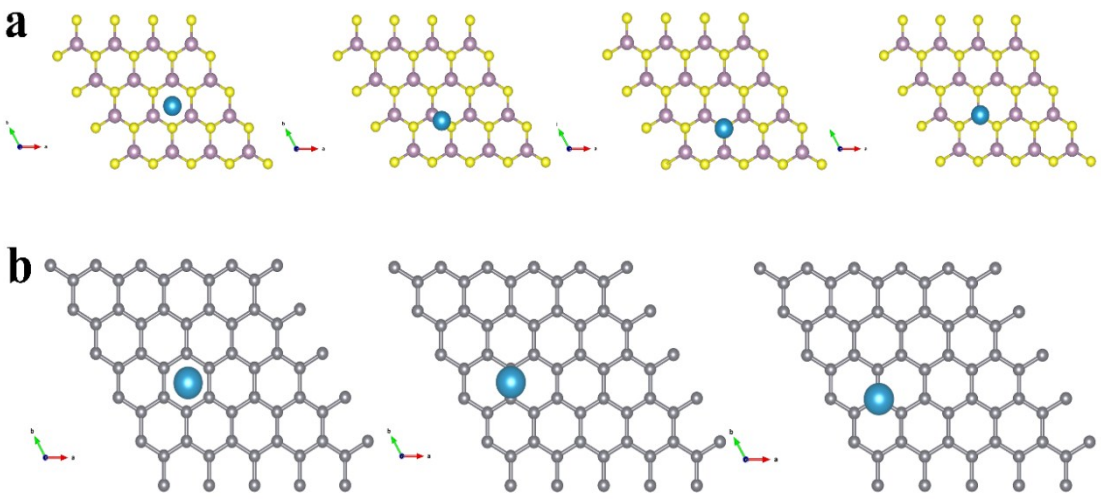


**Fig. S7** (a) Optimized adsorption configurations of Na atom on the hollow, bridge, top

of S atom and top of Mo atom site on the $MoS_2$ layer. (b) Optimized adsorption configurations of Na atom on the hollow, bridge and top of C atom site on the graphene sheet.

**Table S3.** Calculate adsorption energies of Na atom at various active sites of CNT@NCT@W-$MoS_2$/C and CNT@NCT@ $MoS_2$.

| | Active site | $E_{ad}$/eV |
|---|---|---|
| CNT@NCT@$MoS_2$ | Hollow | -0.734 |
| | Bridge | 5.476 |
| | Top-S | 8.479 |
| | Top-Mo | 8.479 |
| CNT@NCT@W-$MoS_2$/C | Hollow | -0.971 |
| | Bridge | -0.999 |

| | | |
|---|---|---|
| | Top-C | -0.937 |

**References**


1 G.B. Xu, L.W. Yang, X.L. Wei, J.W. Ding, P.K. Chu, *Adv. Funct. Mater.,* 2016, **26**, 3349–3358.

2 D.W. Su, S.X. Dou, G.X. Wang, *Adv. Energy Mater.,* 2014, **5,** 1401205.

3 Y.Q. Zhang, H.C. Tao, T. Li, S.L. Du, J.H. Li, Y.K. Zhang, X.L. Yang, *ACS Appl. Mater. Interfaces,* 2018, **10**, 35206-35215.

4 Y. Li, Y. Liang, F.C. Robles Hernandez, H. Deog Yoo, Q. An, Y. Yao, *Nano Energy,* 2015, **15**, 453-461.

5 T.S. Sahu, S. Mitra, *Sci. Rep.,* 2015, **5**, 12571.

6 L. David, R. Bhandavat, G. Singh, *ACS Nano,* 2014, **8**, 1759-1770.

7 X. Xie, Z. Ao, D. Su, J. Zhang, G. Wang, *Adv. Funct. Mater.*, 2015, **25**, 1393-1403.

8 W. Ye, F. Wu, N. Shi, H. Zhou, S. Xiong, *Small,* 2020, **16**, 1906607..

9 Z.T. Shi, W. Kang, J. Xu, L.L. Sun, C.S. Lee, *Small,* 2015, **11**, 5667-5674.

10 H.M. Zhou, P.F. Lv, X.M. Lu, X.B. Hou, Q.F. Wei, *ChemSusChem,* 2019, **12**.